SRTTU

JCARME
ISSN: 2228-7922
Journal of Computational and Applied Research in Mechanical Engineering
Vol. 8, No. 2, pp. 133-144
jcarme.sru.ac.ir

Fuzzy motion control for wheeled mobile robots in real-time

Mohammad Hossein Falsafi, Khalil Alipour* and Bahram Tarvirdizadeh

Advanced Service Robots (ASR) Laboratory, Department of Mechatronics Engineering, Faculty of New Sciences and Technologies, University of Tehran, Tehran, Iran

Article info:
Received: 11/01/2017
Accepted: 02/08/2018
Online: 05/08/2018

Keywords:
Wheeled mobile robot,
Motion control,
Fuzzy logic,
Predictive control.

Abstract
Due to the various advantages of Wheeled Mobile Robots, many researchers have focused on solving their challenges. The automatic motion control of such robots is an attractive problem and is one of the issues which should carefully be examined. In the current paper, the trajectory tracking problem of Wheeled Mobile Robots which are actuated by two independent electrical motors is deliberated. To this end, and also, computer simulation of the system, first, the system model is derived at the level of kinematics. The system model is nonholonomic. Then a simple non-mode-based controller based on fuzzy logic is proposed. The control input resulted from fuzzy logic is then corrected to fulfill the actuation saturation limits and non-slipping condition. To prove the efficiency of the suggested controller, its response, in terms of the required computational time burden and tracking error, is compared with a previously suggested method. The obtained simulation results support the superiority of fuzzy-based method over a previous study in terms of the considered measures.

1. Introduction

In contrast to fixed-base manipulator arms, mobile robots have an unlimited workspace. This advantage stem from the locomotion mechanisms of such robots. The locomotion of such systems can be wheeled, tracked, legged or combination of them [1]. Due to the various advantages of wheeled locomotion, Wheeled Mobile Robots (WMRs) have extensively been studied. To have an autonomous WMR, capable of performing desired tasks, various autonomy challenges including planning and controlling should be solved. As a result, some researchers have tried to design motion controllers to drive the robot to accomplish their favorite missions [2-5].

Motion control of wheeled robots can be divided into three distinct problems. In the first problem, which is called trajectory tracking, it is desired that the robot is controlled such that the desired trajectories of a reference point of the robot be tracked. In the second problem, which is named path following, the control of the robot is aimed at directing the robot in a way that one of its points can follow a desired geometrical path. In the path following problems, the robot velocity along the path is not controlled. In the last problem, which is known as point stabilization,

*Corresponding author
email address: k.alipour@ut.ac.ir

the robot is controlled such that it can reach a desired point with a favorite orientation.

In many studies, it is assumed that the WMR travels with a low velocity and it does not slip laterally and/or longitudinally. This assumption imposes nonholonomic (analytically non-integrable) constraints on the robot motion [6]. Based on Brocket theorem, there is no static smooth feedback of state variables for the point stabilization [7]. Hence, various control methods have been presented to stabilize WMRs which can be categorized into continuous and discontinuous time controllers. Samson developed smooth continuous-time controllers well while the discontinuous controllers were studied in [8, 9].

Motion control of robots can be classified into two kinematical and dynamical schemes. In the kinematic controllers, the input controls are angular velocities of wheels while dynamic controllers are designed by considering the actuating torques of wheels as the adjustable input control.

Considering parametric uncertainties, an adaptive controller was suggested for a group of nonholonomic mechanical systems at the level of dynamics [10]. Ge et al. [11] examined stabilization of chained systems using a robust adaptive algorithm while parametric uncertainties and external disturbance were considered. The trajectory tracking of a two-wheeled robot was examined using the backstepping technique, while non-parametric uncertainties and disturbances were taken into account [12]. Dong et al. [13] designed an adaptive backstepping controller for both trajectory tracking and point stabilization A robust controller was suggested to exponentially stabilizing of WMRs containing parametric uncertainties [14]. An adaptive controller was suggested for WMRs where the motor dynamics was furthermore considered [15]. The adaptive sliding mode controller was suggested to track the designated trajectories in [16].

In addition to the works focused on controlling a WMR containing a single platform, some researchers were just recently addressed controlling a WMR including two platforms [17-19]. In these works, using actuators of tractor platform, the motion of trailer platform, whose wheels are passive, was controlled.

In most of the above-mentioned studies, the control law was devised based on the accurate model or the model with some uncertainties. The control laws which depend on the model suffer from several drawbacks. Therefore, the first contribution of the current paper is utilizing Fuzzy Control (FC) method, which is a non-model based controller, to the tracking-error control of the differentially-driven WMR. The second benefit of the present research is the assessment of the proposed FC-based algorithm versus the work done by Gregor, and Igor [2]. The benefits of the developed FC over the Model Predictive Control (MPC) are examined in the current study. Besides, the performances of the FC versus MPC in trajectory tracking of the WMR are analyzed from two points of view. The first one is the path tracking error and the second one is the processing time duration.

After this introduction, the remainder of the present study is organized as described. In the next section, the model of WMR at the level of kinematics is rendered which is followed, in section 3, by some prerequisite material required for its motion control. Then, the suggested fuzzy based method and model predictive one are introduced in detail in sections 4 and 5, correspondingly. In succeeding section, the obtained results of the forgoing control techniques are compared. The conclusions of the paper will be addressed in the last section.

2. Modeling of WMR

In the present section, the kinematics model of the robot system is detailed. Then, the control problem regarding trajectory tracking of the robot is defined.

2.1. WMR kinematic model

The robotic system which is to be modeled consists of two active wheels and a single passive wheel. The passive wheel is added to the robot platform to improve its stability. To derive the system kinematics, two frames are attached to the mobile platform as depicted in Fig. 1. The $Z - \Upsilon$ presents the world-coordinate frame while

$\rho-\upsilon$ denotes its body-coordinate frame which is completely attached to the robot and travels with it. The two active wheels are actuated by two independent electrical DC motors. The considered motors can provide the commanded feasible angular velocity. It should be noted that the passive wheel is a kind of caster or spherical type. Notice that while the number of passive wheels may affect the postural stability of the system, it does not change the kinematics of it. The robot center of mass is located at point G while point O denotes the mid-point of the line connecting the center of two active wheels. The distance between point O and G is considered as *b* (Fig. 1). In the current study, for the sake of simplicity, *b* is considered as zero. The robot pose is represented by coordinates of one of its points and the heading angle ϑ. It is also worth mentioning that the origin of coordinates $\rho-\upsilon$ frame relative to $Z-\Upsilon$ frame is denoted by (Z_0, Υ_0). Likewise, the coordinates of point G in inertial frame are represented as (Z_G, Υ_G). The distance between the active wheels center is considered as D. The rotational velocities of right and left wheels around their axels are represented by Ω_R and Ω_L, respectively. Moreover, the wheels radius is denoted as κ.

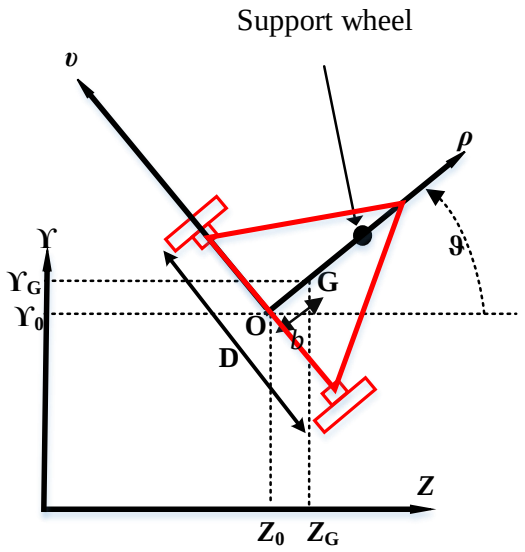

Fig. 1. The three-wheeled robot configuration along with its geometrical parameters.

The robot configuration parameters are denoted by vector $\boldsymbol{\mu}=[Z_G \quad \Upsilon_G \quad \vartheta]^T$. In the current research, it is supposed the robot moves on a flat terrain. Also, the robot, wheels, as well as terrain are assumed to be rigid. Wheels are subjected to pure rolling. This means that the robot wheels do not slip either laterally or longitudinally. Based on Fig. 2, if the angular velocity of the robot is represented by $\boldsymbol{\Omega}$, then the linear velocity of the robot wheels center can be written as follows:

$$\mathbf{S_R} = \mathbf{S_o} + \boldsymbol{\Omega} \times \mathbf{d_{R/O}} \tag{1}$$

$$\mathbf{S_L} = \mathbf{S_o} + \boldsymbol{\Omega} \times \mathbf{d_{L/O}} \tag{2}$$

where $\mathbf{S_R}$ and $\mathbf{S_L}$ indicate the linear velocity of the right and left wheels center, respectively. Besides, $\mathbf{S_O}$ represents the point O linear velocity. Also, $\mathbf{d_{R/O}}$ and $\mathbf{d_{L/O}}$ indicate the position of the right and left wheels center relative to point O, respectively.

If the unit vectors of the robot body coordinate frame along ρ, υ and η directions are considered as $\mathbf{u_1}$, $\mathbf{u_2}$ and $\mathbf{u_3}$, respectively, then the following relations can be written:

$$S_R\mathbf{u_1} = S.\mathbf{u_1} + (\Omega.\mathbf{u}_3) \times (-\frac{D}{2}\mathbf{u}_2) \tag{3}$$

$$S_L\mathbf{u_1} = S.\mathbf{u_1} + (\Omega.\mathbf{u}_3) \times (\frac{D}{2}\mathbf{u}_2) \tag{4}$$

In the above equations, S_R and S_L denote the speed of the right and left wheels center, correspondingly. Moreover, '×' indicates the operator of the vector outer product.

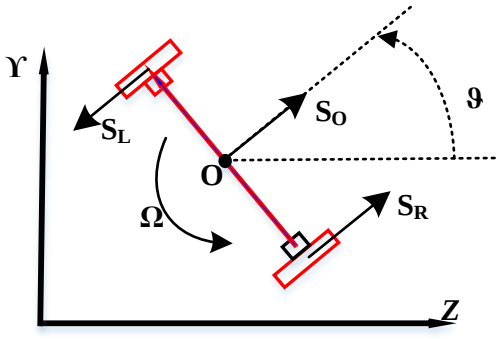

Fig. 2. The kinematic diagram of the DDWMR.

Using the last two relations, one can obtain the following equation:

$$\begin{cases} S_R = S + \Omega.\dfrac{D}{2} \\ S_L = S - \Omega.\dfrac{D}{2} \end{cases} \Rightarrow \begin{bmatrix} S \\ \Omega \end{bmatrix} = \kappa \begin{bmatrix} 1/2 & 1/2 \\ 1/D & -1/D \end{bmatrix} \begin{bmatrix} \Omega_R \\ \Omega_L \end{bmatrix} \quad (5)$$

According to the above equation, one can claim that a one-to-one relationship exists between the actual input controls of the robot, namely Ω_R and Ω_L , and its linear/angular velocity. Hence, instead of robot rotational velocities, one can easily utilize S and Ω as the control input, as will be observed in Section 4.

As mentioned previously, the robot wheels do not slip. Hence, the point O linear velocity will simply be in the ρ axis direction. Therefore, it can be concluded that $\dot{Z}_G = S \cdot c(\vartheta)$ and $\dot{\Upsilon}_G = S \cdot s(\vartheta)$ in which *s*() and *c*() stand for sin() and cos() functions, respectively. If the relation $\dot{\vartheta} = \Omega$ is added to the equations denoting the two components of linear velocity of point O, then the following vector/matrix equation results:

$$\dot{\boldsymbol{\mu}} = \begin{bmatrix} c(\vartheta) & 0 \\ s(\vartheta) & 0 \\ 0 & 1 \end{bmatrix} \begin{bmatrix} S \\ \Omega \end{bmatrix} \quad (6)$$

2.2. Maximum translational and rotational speeds

To address the issue of actuators limitations in the controller design process, the process proposed by Gregor, and Igor [2] is followed. Herein, this technique is elaborated. In this process, it is required that the maximum translational and rotational speeds of the robot that can be produced by actuators are computed according to the extreme angular velocities of the motors. If the extreme rotational velocity of the wheels is denoted by $\varpi_{\max}$, then one can claim that the maximal linear velocity of the WMR is generated when two motorized wheels are rotating with $\varpi_{\max}$. Consequently, the following equation can be written:

$$\begin{cases} S = \dfrac{\Omega_R + \Omega_L}{2}\kappa \\ \Omega_R = \Omega_L = \varpi_{\max} \end{cases} \Rightarrow S_{\max} = \varpi_{\max} \cdot \kappa \quad (7)$$

Likewise, once the two motorized wheels are in motion in contrast directions with maximum angular velocity, the maximal angular velocity is resulted. Therefore, the following result is obtained.

$$\begin{cases} \Omega = \dfrac{\Omega_R - \Omega_L}{D} \times \kappa \\ \Omega_R = -\Omega_L = \omega_{\max} \end{cases} \Rightarrow \Omega_{\max} = 2\omega_{\max}\frac{\kappa}{D} \quad (8)$$

By defining the factor α based on the ratio of translational/rotational speeds, and the maximum $\Omega_{\max}/S_{\max}$, as follows, the initial control command can be corrected as:

$$\begin{aligned} &\text{I) } S_c > S_{\max} \Rightarrow \alpha = \frac{|S|}{S_{\max}} \Rightarrow \\ &\qquad S_c = \text{sign}(S).S_{\max},\ \Omega_c = \frac{\Omega}{\alpha} \\ &\text{II) } \Omega_c > \Omega_{\max} \Rightarrow \alpha = \frac{|\Omega|}{\Omega_{\max}} \Rightarrow \\ &\qquad S_c = \frac{S}{\alpha},\ \Omega_c = \text{sign}(\Omega).\Omega_{\max} \\ &\text{III) } S_c < S_{\max},\ \Omega_c < \Omega_{\max} \Rightarrow \\ &\qquad \alpha = 1 \Rightarrow S_c = S,\ \Omega_c = \Omega \\ &\alpha = \max\left\{\frac{|S|}{S_{\max}},\ \frac{|\Omega|}{\Omega_{\max}},\ 1\right\} \end{aligned} \quad (9)$$

It should be emphasized that the above relations can be resulted based on the point that if one of the linear or rotational speed is modified, the other one should also be corrected so as the curvature radius of the path traveled by the WMR can be kept [2]. Note that in the above relations, sign(.) denotes the function of signum. In addition to the above modifications of the control inputs, to avoid the robot slipping, the robot acceleration should not be exceeded some specified threshold (represented by be β_{max}), [2]. To address the wheeled robot acceleration constraint, according to the definition of the acceleration, one should pay attention to the

robot velocity history. Hence, the following equations can be written:

$$\begin{cases} |\beta_R| \le \beta_{\max} \Rightarrow \quad S_{Rc} = S_R(i) \\ |\beta_R| \ge \beta_{\max} \Rightarrow \\ \quad S_{Rc}(i) = S_R(i-1) + \\ \quad \text{sign}(\beta_R).\beta_{\max}.S_s \end{cases} \qquad (10)$$

$$\begin{cases} |\beta_L| \le \beta_{\max} \Rightarrow \quad S_{Lc} = S_L(i) \\ |\beta_L| \ge \beta_{\max} \Rightarrow \quad S_{Lc}(i) = \\ \quad S_L(i-1) + \text{sign}(\beta_L).\beta_{\max}.S_s \end{cases}$$

Note that in the above relations, β_R and β_L represent the acceleration of the right and left wheels centers, accordingly. In addition, S_{Rc} and S_{Lc} indicate the linear control command associated with the WMR right and left wheels, respectively. Moreover, S_s represents the sampling time. It is worth to mention that β_{max}, which can be computed experimentally, is strongly intertwined with the features of the robot actuators.

3. Reference trajectories and tracking errors

In the current section, some of the material required for the controller design is introduced. To this end, a virtual robot which is called reference robot and tracks ideally the robot desired trajectories is considered (Fig. 3). Based on this concept, the tracking errors of the real robot along with the robot attached frame can be obtained considering the tracking errors in the $Z-\Upsilon$ frame as:

$$\begin{cases} \varepsilon_Z = Z_r - Z_0 \\ \varepsilon_\Upsilon = \Upsilon_r - \Upsilon_0 \end{cases} \Rightarrow \begin{cases} \varepsilon_1 = \varepsilon_Z.c(\vartheta) + \varepsilon_\Upsilon.s(\vartheta) \\ \varepsilon_2 = -\varepsilon_Z.s(\vartheta) + \varepsilon_\Upsilon.c(\vartheta) \end{cases} \qquad (11)$$

Note that Z_r and Υ_r represent the reference trajectories of the robot in the direction of Z and Υ, correspondingly. Besides, ε_Z and ε_Υ represent the tracking error of the robot along Z and Υ axes, respectively. Moreover, ε_1 and ε_2 characterize the WMR tracking errors in the $\rho-\upsilon$ frame.

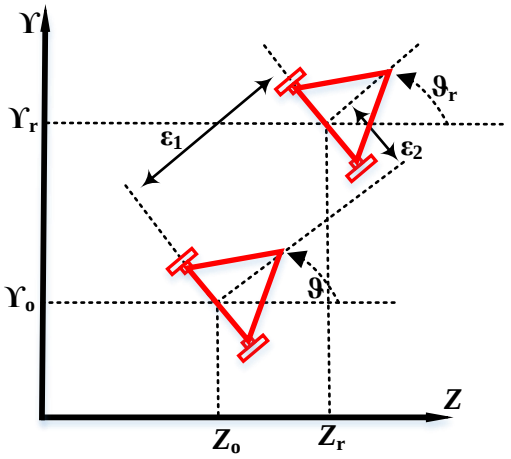

Fig. 3. The DDWMR tracking error schematic.

By adding the equation $\varepsilon_3 = \vartheta_r - \vartheta$, to Eq. (11), the subsequent matrix/vector equation can be achieved.

$$\boldsymbol{\varepsilon} = \begin{bmatrix} c(\vartheta) & s(\vartheta) & 0 \\ -s(\vartheta) & c(\vartheta) & 0 \\ 0 & 0 & 1 \end{bmatrix} (\boldsymbol{\mu}_r - \boldsymbol{\mu}) \qquad (12)$$

where $\boldsymbol{\mu}_r$ represents the WMR reference pose vector. It is worth mentioning that in addition to the controller performance, the tracking errors of the robot rely on two additional factors. One of the foregoing factors is the initial values of the tracking errors, namely entities of $|\boldsymbol{\mu}_0 - \boldsymbol{\mu}_{r0}|$, where $\boldsymbol{\mu}_0$ and $\boldsymbol{\mu}_{r0}$ represent the beginning actual and reference robot pose, respectively. The other factor is the sampling frequency, i.e. the inverse of S_s, utilized in the implementing of the designed controller. The smaller values of these two factors can result in better tracking performance of the robot. Note that the higher values of the sampling frequency can result in the better performance provided that no restriction exists in the real-time computations.

4. Fuzzy controller design

Based on the introductory explanations rendered in the previous section, here the design of the fuzzy controller is presented. As will be seen later, the embedded fuzzy rules depend on additional two errors called range and heading-angle errors. These two errors are defined as:

$$\varepsilon_b = \sqrt{\varepsilon_1^2 + \varepsilon_2^2} \quad (13)$$

$$\varepsilon_\vartheta = \tan^{-1}(\varepsilon_2/\varepsilon_1) \quad (14)$$

where ε_b specifies the range error, and ε_ϑ indicates the heading error. To generate the control signals based on the developed fuzzy method, first the errors ε_Z and ε_Υ should be converted to ε_b and ε_ϑ. In this regard, a block is considered in the block-diagram of the suggested control method, as can be observed in Fig. 4. The developed fuzzy controller generates the WMR input signals, S and Ω, based on ε_b and ε_ϑ. It should be pointed out that the robot can compensate the distance error by the linear velocity and the angular error by the angular velocity. Hence, the controller design based on ε_b and ε_ϑ is beneficial. Indeed, adopting these errors removes the cross-coupling problem once the rule-base is generated. As a result, composing the fuzzy rules is simplified.

A fuzzy-based controller consists of various features. The first feature is called fuzzification. This feature is formed based on membership functions (MFs) and by which a crisp value is transformed to a fuzzy value. The second element of a fuzzy controller is named rule-base and consists of a set of "if-then" rules. The third part of a fuzzy controller is known as defuzzification which converts a fuzzy value to a crisp value. Fig. 5 to 8 describe the MFs for ε_b, ε_ϑ, S and Ω, correspondingly. Note that the whole aforementioned MFs are obtained by adopting trial and error approach.

The value of WMR translational velocity is categorized into several Linguistic Variables (LVs) as depicted in Table 1. This table also states the linguistic variables of range error ε_b. Besides, in Table 2, the linguistic variables associated with WMR rotational velocity and the heading error ε_ϑ are given.

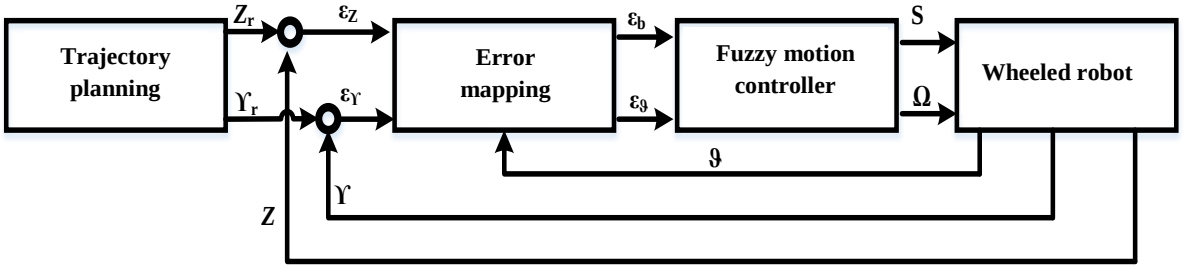

Fig. 4. The developed fuzzy control algorithm.

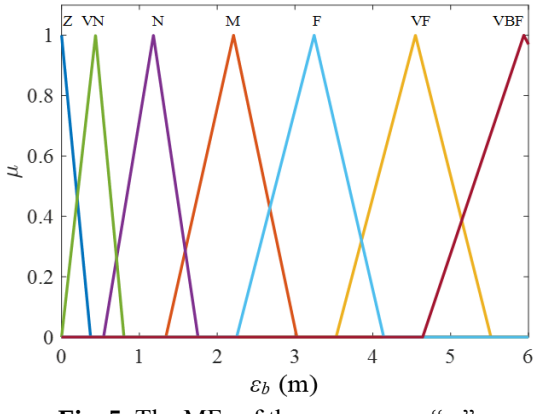

Fig. 5. The MFs of the range error "ε_b".

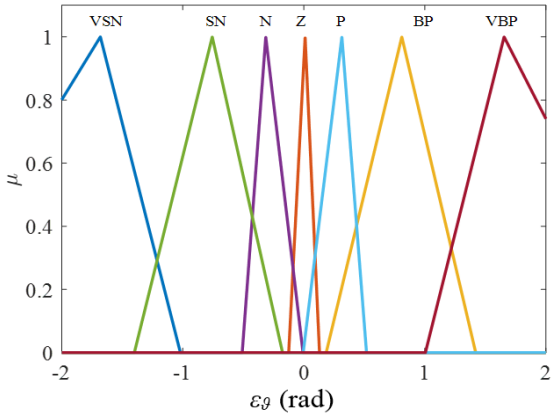

Fig. 6. The MFs of the heading error "ε_ϑ".

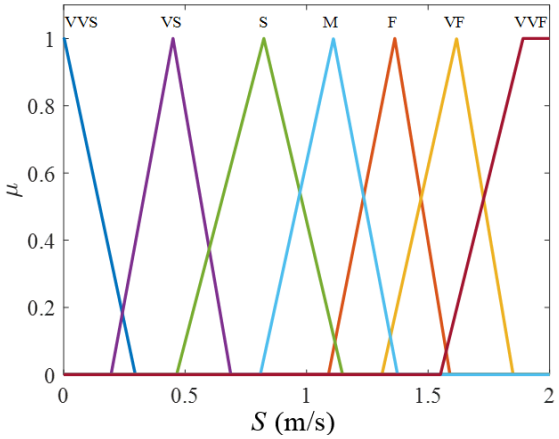

Fig. 7. The MFs of the linear velocity "S".

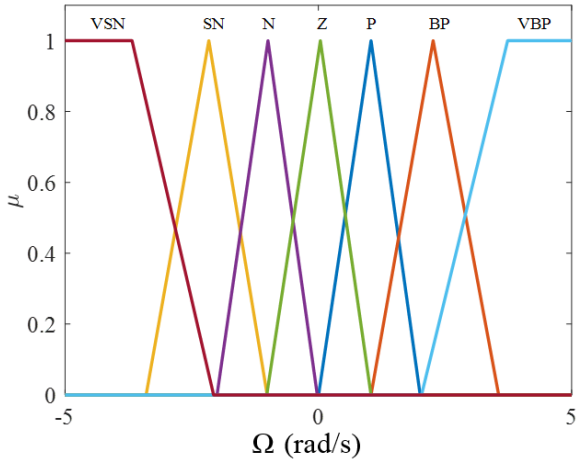

Fig. 8. The MFs of the rotational velocity "Ω".

Table 1. The LVs for WMR translational speed and range error ε_b.

The LVs associated with S	The LVs associated with WMR range error
VVS →Very very slow	Z→Zero
VS→Very slow	VN→Very near
S→Slow	N→Near
M→Medium	M→Medium
F→Fast	F→Far
VF→Very fast	VF→Very far
VVF→Very very fast	VBF→Very big far

Table 2. The LVs for WMR rotational speed and heading error ε_ϑ.

The LVs associated with Ω	The LVs associated with WMR heading error
VSN→ Very small negative	VSN→Very small negative
SN→ Small negative	SN→ Small negative
N→ Negative	N→ Negative
Z→ Zero	Z→ Zero
P→ Positive	P→ Positive
BP→ Big positive	BP→ Big positive
VBP→ Very big positive	VBP→ Very big positive

In Table 3, the employed rule-bases are reflected. It is worth mentioning that in the present study, the fuzzy inference system is of type Mamdani [20]. In addition, for the output-defuzzification purposes, the method of "centroid" is exploited.

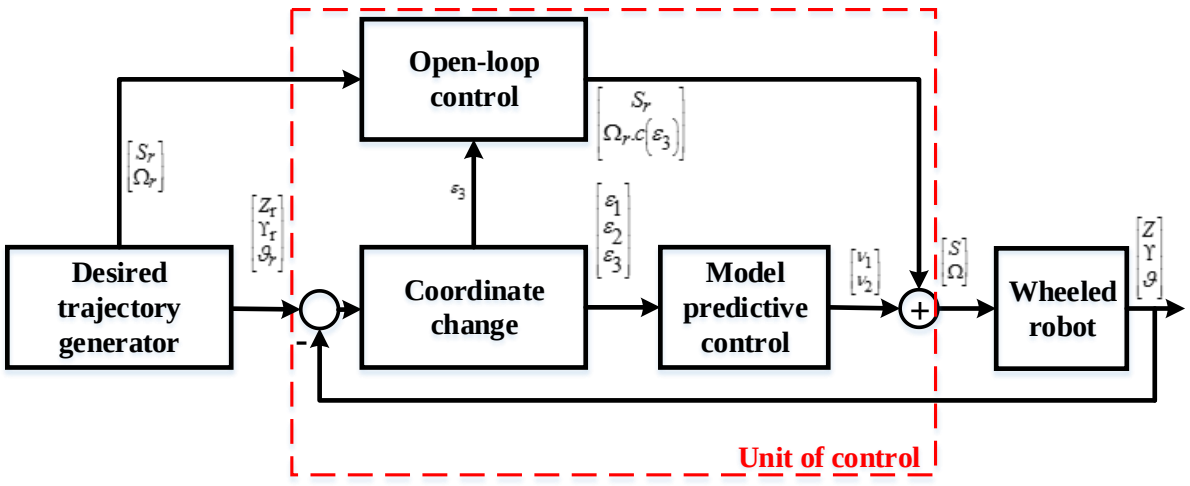

Fig. 9. The control topology utilized by Klančar, and Škrjanc [2] to motion control of the WMRs.

Table 3. The utilized rule-base for constructing WMR control inputs.

The FC rule-bases for S	The FC rule-bases for Ω
If ε_b is Z then S is VVS	If ε_ϑ is VSN then Ω is VSN
If ε_b is VN then S is VS	If ε_ϑ is SN then Ω is SN
If ε_b is N then S is S	If ε_ϑ is N then Ω is N
If ε_b is M then S is M	If ε_ϑ is Z then Ω is Z
If ε_b is F then S is F	If ε_ϑ is P then Ω is P
If ε_b is VF then S is VF	If ε_ϑ is BP then Ω is BP
If ε_b is VBF then S is VVF	If ε_ϑ is VBP then Ω is VBP

5. An overview of MPC design

To study the response of the suggested controller, in terms of tracking performance and the required computational time, an attractive control strategy based on MPC is utilized. In the present study, the MPC controller, presented by Gregor, and Igor [2], to adjust the motion of WMRs is exploited. Therefore, in the present section, this control method is summarized. Fig. 9 illustrates the presented control topology. The aforementioned controller is realized based on the combination of two open- and closed-loop controls. In fact, like many tracking controllers, some of the nonlinearities are canceled by adopting feedforward strategy, and the system is prepared for fine tuning by MPC-based closed-loop. Consequently, the vector of WMR control input $\boldsymbol{\nu}$ can be written as:

$$\boldsymbol{\nu} = \boldsymbol{\nu}_{FF} + \boldsymbol{\nu}_{FB} \tag{15}$$

where $\boldsymbol{\nu}_{FF}$ and $\boldsymbol{\nu}_{FB}$ represent the open-loop (feedforward) and closed-loop slices of the control signal, correspondingly.
To calculate the feedforward control signal, first, the translational and rotational angular velocities, as well as the reference heading angle of WMR, should be calculated. The aforementioned quantities can be attained as:

$$S_r = \pm\sqrt{\dot{Z}_r^{\,2} + \dot{\Upsilon}_r^{\,2}} \tag{16}$$

$$\vartheta_r = A\tan 2(\dot{\Upsilon}_r, \dot{Z}_r) + i\pi \tag{17}$$

$$\Omega_r = \frac{\dot{Z}_r.\ddot{\Upsilon}_r - \dot{\Upsilon}_r.\ddot{Z}_r}{\dot{Z}_r^2 + \dot{\Upsilon}_r^2} \tag{18}$$

In the above equation, S_r, ϑ_r and Ω_r represent the favorite translational speed, desired orientation and reference rotational speed, correspondingly. According to these factors, the feedforward signal, $\boldsymbol{\nu}_{FF}$, can be written as follows:

$$\boldsymbol{\nu}_{FF} = [S_r \quad \Omega_r.c(\varepsilon_3)]^T \tag{19}$$

After obtaining the feedforward signal, the feedback signal is derived. To this end, first, the error dynamics is obtained. In this direction, Eq. (12) is differentiated with respect to the time which leads to the following relation:

$$\dot{\boldsymbol{\varepsilon}} = \begin{bmatrix} -\dot{\vartheta}\mathrm{s}(\vartheta) & \dot{\vartheta}\mathrm{c}(\vartheta) & 0 \\ -\dot{\vartheta}\mathrm{c}(\vartheta) & -\dot{\vartheta}\mathrm{s}(\vartheta) & 0 \\ 0 & 0 & 0 \end{bmatrix}(\boldsymbol{\mu}_r - \boldsymbol{\mu}) + \begin{bmatrix} \mathrm{c}(\vartheta) & \mathrm{s}(\vartheta) & 0 \\ -\mathrm{s}(\vartheta) & \mathrm{c}(\vartheta) & 0 \\ 0 & 0 & 1 \end{bmatrix}(\dot{\boldsymbol{\mu}}_r - \dot{\boldsymbol{\mu}}) \tag{20}$$

Now, according to Eq. (6), terms $\dot{\boldsymbol{\mu}}$ and $\dot{\boldsymbol{\mu}}_r$ are substituted which leads to the next equation:

$$\dot{\boldsymbol{\varepsilon}} = \begin{bmatrix} -\dot{\vartheta}\mathrm{s}(\vartheta) & \dot{\vartheta}\mathrm{c}(\vartheta) & 0 \\ -\dot{\vartheta}\mathrm{c}(\vartheta) & -\dot{\vartheta}\mathrm{s}(\vartheta) & 0 \\ 0 & 0 & 0 \end{bmatrix}(\boldsymbol{\mu}_r - \boldsymbol{\mu}) + \begin{bmatrix} \mathrm{c}(\vartheta - \vartheta_r) & 0 \\ -\mathrm{s}(\vartheta - \vartheta_r) & 0 \\ 0 & 1 \end{bmatrix}\begin{bmatrix} S_r \\ \Omega_r \end{bmatrix} + \begin{bmatrix} -1 & 0 \\ 0 & 0 \\ 0 & -1 \end{bmatrix}\boldsymbol{\nu} \tag{21}$$

By substituting Eq. (15) for $\boldsymbol{\nu}$ and considering Eq. (19), the following equation is obtained:

$$\dot{\boldsymbol{\varepsilon}} = \begin{bmatrix} 0 & \Omega & 0 \\ -\Omega & 0 & 0 \\ 0 & 0 & 0 \end{bmatrix}\boldsymbol{\varepsilon} + \begin{bmatrix} 0 \\ \mathrm{s}(\varepsilon_3) \\ 0 \end{bmatrix} S_r + \begin{bmatrix} -1 & 0 \\ 0 & 0 \\ 0 & -1 \end{bmatrix}\boldsymbol{\nu}_{FB} \tag{22}$$

Note that the above equation is obtained considering $\varepsilon_3 = \vartheta_r - \vartheta$ and linearizing the error dynamics around the reference trajectory

($\varepsilon_1=\varepsilon_2=\varepsilon_3=0$). After that, the following consequences are achieved:

$$\dot{\boldsymbol{\varepsilon}} = \mathbf{A}_{cls}\boldsymbol{\varepsilon} + \mathbf{B}_{cls}\mathbf{v}_{\mathbf{FB}} \tag{23}$$

In the above equation, $\mathbf{A}_{cls}$ and $\mathbf{B}_{cls}$ are:

$$\mathbf{A}_{cls} = \begin{bmatrix} 0 & \Omega_r & 0 \\ -\Omega_r & 0 & S_r \\ 0 & 0 & 0 \end{bmatrix},$$
$$\mathbf{B}_{cls} = \begin{bmatrix} -1 & 0 \\ 0 & 0 \\ 0 & -1 \end{bmatrix} \tag{24}$$

The above differential vector equation can be transformed into different equation as:

$$\begin{aligned} &\boldsymbol{\varepsilon}(i+1) = \mathbf{A}\,\boldsymbol{\varepsilon}(i) + \mathbf{B}\,\mathbf{v}_{\mathbf{FB}}(i) \\ &\mathbf{A} = (\mathbf{I} + \mathbf{A}_{cls}S_s),\ \mathbf{B} = \mathbf{B}_{cls}S_s \end{aligned} \tag{25}$$

According to the above linear equation, designing an MPC is possible. To this end, a quadratic performance index representing the tracking error and control effort is established as:

$$\Pi(\mathbf{v}_{\mathbf{B}}, i) = \sum_{i=1}^{h} \begin{pmatrix} \mathbf{e}^T(i,j).\mathbf{W}.\mathbf{e}(i,j) + \\ \mathbf{v}_{\mathbf{B}}^{\mathbf{T}}(i,j).\mathbf{T}.\mathbf{v}_{\mathbf{B}}(i,j) \end{pmatrix} \tag{26}$$

Notice that in Eq. (26), h indicates the time horizon. Also, $\mathbf{e}(i,j) = \boldsymbol{\varepsilon}_{\mathbf{r}}(k+j) - \boldsymbol{\varepsilon}(i+j\,|\,i)$, in which $\boldsymbol{\varepsilon}_{\mathbf{r}}(i+j)$ characterizes the reference WMR error. Besides, $\boldsymbol{\varepsilon}(i+j\,|\,i)$ denotes the estimated error of the actual WMR at sample time of $(i+j)$ according to the data of the first i sampling periods. Also, $\mathbf{W}$ is a square semi positive matrix with dimension n. Likewise, $\mathbf{T}$ characterizes a square positive definite scaling matrix with dimension m. It is pointed out that in the current study, the value of n is set as 3 while m is equal to 2. The closed-loop part of the control input signal, $\mathbf{v}_{\mathbf{B}}$, is attained by extremizing the aforementioned performance index Π, as:

$$\mathbf{v}_{FB}(i) = \mathbf{F}_{mpc}\boldsymbol{\varepsilon}(i) \tag{27}$$

in which $\mathbf{F}_{mpc}$ is calculated according to the next equations:

$$\mathbf{F}_{mpc} = \left(\mathbf{H}^{\mathbf{T}}\overline{\mathbf{Q}}\,\mathbf{H} + \overline{\mathbf{T}}\right)^{-1}\mathbf{H}^{\mathbf{T}}\overline{\mathbf{W}}\left(\mathbf{v}_{\mathbf{r}} - \mathbf{v}\right) \tag{28}$$

where

$$\mathbf{H}(i) = \begin{bmatrix} \mathbf{B}(i\,|\,i) & 0 & \cdots & 0 \\ \mathbf{A}(i+1\,|\,i).B(i/i) & \mathbf{B}(i+1\,|\,i) & \cdots & \vdots \\ \vdots & \vdots & \ddots & \vdots \\ \boldsymbol{\Delta}(i,1).B(i\,|\,i) & \boldsymbol{\Delta}(i,2).\mathbf{B}(i+1\,|\,i) & \cdots & \mathbf{B}(i+h-1\,|\,i) \end{bmatrix}$$
$$\boldsymbol{\Delta}(i,j) = \prod_{k=j}^{h-1}\mathbf{A}(i+k\,|\,i)$$
$$\overline{\mathbf{W}}_{(\mathrm{h.n})\times(\mathrm{h.n})} = \begin{bmatrix} W & 0 & \cdots & 0 \\ 0 & W & \cdots & 0 \\ \vdots & \vdots & \ddots & \vdots \\ 0 & 0 & \cdots & W \end{bmatrix}$$
$$\overline{\mathbf{T}}_{(\mathrm{h.m})\times(\mathrm{h.m})} = \begin{bmatrix} T & 0 & \cdots & 0 \\ 0 & T & \cdots & 0 \\ \vdots & \vdots & \ddots & \vdots \\ 0 & 0 & \cdots & T \end{bmatrix} \tag{29}$$
$$\mathbf{v}(k) = \left[\mathbf{A}(i\,|\,i) \quad \mathbf{A}(i+1\,|\,i).\mathbf{A}(i\,|\,i) \quad .... \quad \boldsymbol{\Delta}(i,0)\right]^T$$
$$\mathbf{v}_r = \left[\mathbf{A}_r \quad \mathbf{A}_r^2 \quad .... \quad \mathbf{A}_r^h\right]^T$$
$$\boldsymbol{\varepsilon}_r(i+1) = \mathrm{A}_r^j(i).\boldsymbol{\varepsilon}(i), \qquad j=1,\ldots,h$$

6. The response of the suggested fuzzy based controller against MPC

To assess the response of the proposed controller against MPC, various maneuvers can be considered. In the present section, the response of one of these maneuvers will be detailed. The supposed favorite trajectories in the inertial coordinate frame for the robot to track is:

$$\begin{cases} Z_r = 1.1 + 0.7 \times \mathrm{s}(0.209t) \\ \Upsilon_r = 0.9 + 0.7 \times c(0.4189t) \end{cases} \tag{30}$$

in which, $t = [0 \sim 30]$ sec. Also, the sampling time S_s is set as 0.1 sec. The performance of the fuzzy control based method and that of MPC is examined in terms of two measures. The first important vector addresses the trajectory

tracking precision while the next one requires processing time duration. For the supposed maneuver, it is assumed that the robot initiates its motion with an initial distance to the desired trajectories. Besides, due to the real-world conditions and actuator limitations, it is assumed that the extreme translational and rotational accessible speeds are S_{MAX}=0.5m/s and Ω_{MAX}=13rad/s. In addition, to avoid the robot wheels from slipping, it is also assumed that the wheels translational acceleration is at most β_{MAX} = 3m/s^2.

6.1. Trajectory tracking error assessment

In this subsection, the performance of the two controllers are explored in terms of tracking precision. In this regard, the simulation results obtained are depicted in Figs. 10 and 11.
As observed, while both controllers can lead to the successful tracking of WMR, the fuzzy-based controller can push the robot to the prescribed trajectories sooner as compared to the MPC. The total tracking error is computed for the two mentioned controllers using the following equation:

$$Error = \sum_{t=t_{initial}}^{t=t_{ultimate}} \left(\left| Z(t) - Z_r(t) \right| + \left| \Upsilon(t) - \Upsilon_r(t) \right| \right) \quad (31)$$

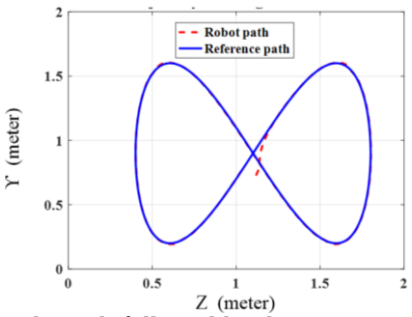

Fig. 10. The path followed by the WMR employing the fuzzy- based method.

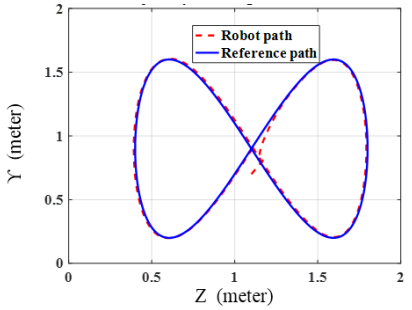

Fig. 11. The path followed by the WMR employing the model predictive method.

In Table 4, the response of the two controllers is presented. As seen in this table, the magnitude of tracking error resulted using fuzzy-based technique is less than that originated from MPC.

Table 4. The error resulted from two control methods for the prescribed trajectories.

Method of control	Fuzzy	Model predictive
Error quantity	27.02	37.50

6.2. Required processing time duration

In Fig. 12 and Fig. 13 the required processing time durations, by the central processor, for the both of the fuzzy and the model predictive controllers are demonstrated which are 0.015 (s) and 0.3 (s) in FC and MPC, respectively. This means that the FC can produce the output signals for about 20 times faster than the MPC.

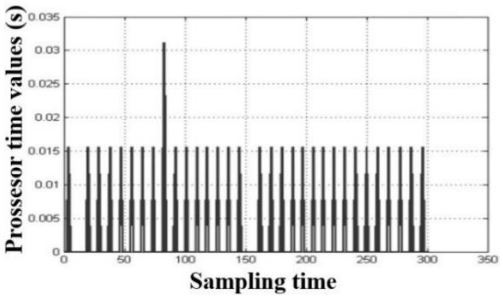

Fig. 12. Processing time for fuzzy model.

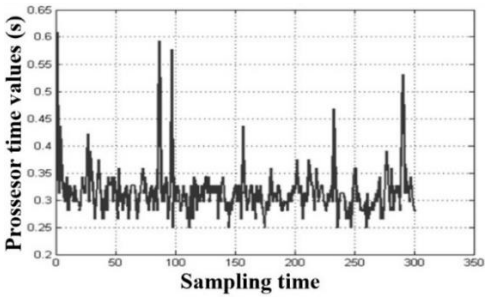

Fig. 13. Processing time for MPC.

In addition, the minimum value of the processing time duration limits the minimum value of the sampling time/discretization period. Consequently, the controller processing speed affects the system control performance, implicitly. Considering this point, it can be concluded that the FC performance can be increased as compared with the MPC. The control inputs of the FC and MPC are demonstrated in Fig. 14 and Fig. 15, respectively. As seen, while the angular velocity signal of MPC is better than that of FC, both controllers are successfully fulfilled the limitation

considered for this control input. Additionally, the linear velocity input of FC seems to be better than that of MPC. However, again both controllers are satisfied their actuator saturation constraints, based on Eqs. (9 and 10).

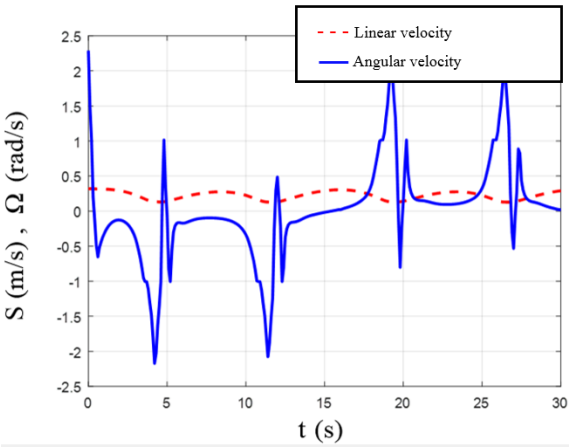

Fig. 14. Linear and angular velocities in FC.

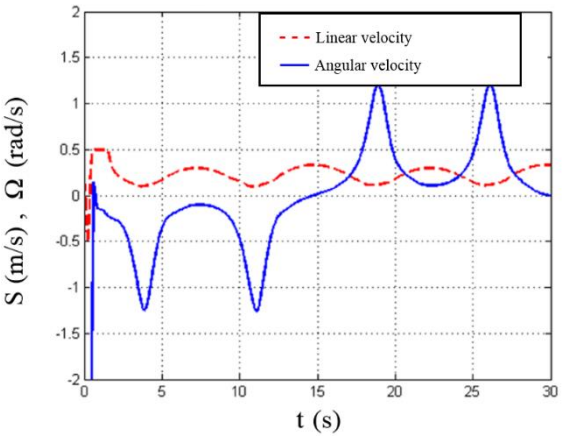

Fig. 15. Linear and angular velocities in MPC.

7. Conclusions

In the current research, a fuzzy-based method is suggested for the trajectory tracking control of WMRs. The considered 3-wheeled robot contains two motorized wheels along with a passive wheel. To simulate the system response and design a kinematical controller, the model of the robot at the level of kinematics is derived. Next, a simple but efficient fuzzy controller is designed, and its response is examined against a model predictive controller in terms of two points of view. The first criterion is the tracking accuracy and the second one is the required processing time durations. The achieved simulation results reveal the superior behavior of the fuzzy-based method against MPC in terms of both aforementioned performance indices.

References

[1] L. Bruzzone, and Quaglia Giuseppe, "Locomotion systems for ground mobile robots in unstructured environments." *Mechanical Sciences* Vol. 3, No. 2, pp. 49-62, (2012).

[2] Gregor Klančar, and Igor Škrjanc. "Tracking-error model-based predictive control for mobile robots in real time." *Robotics and Autonomous Systems*, Vol. 55, No. 6, pp.460-469, (2007).

[3] Tian Yu, and Nilanjan Sarkar, "Control of a mobile robot subject to wheel slip." *Journal of Intelligent & Robotic Systems*, Vol. 74, No. 3-4, pp. 915-929, (2014).

[4] Hadi Amoozgar, Mohammad Khalil Alipour, and Seyed Hossein Sadati, "A fuzzy logic-based formation controller for wheeled mobile robots." *Industrial Robot: An International Journal*, Vol. 38, No. 3 pp. 269-281, (2011).

[5] Khalil Alipour, and S. Ali A. Moosavian, "Dynamically stable motion planning of wheeled robots for heavy object manipulation." *Advanced Robotics*, Vol. 29, No. 8, pp. 545-560, (2015).

[6] Kevin M. Lynch, and C. Park Frank, *Modern Robotics: Mechanics, Planning, and Control*, Cambridge University Press, (2017).

[7] Anthony M. Bloch, Mahmut Reyhanoglu, and N. Harris McClamroch, "Control and stabilization of nonholonomic dynamic systems." *IEEE Transactions on Automatic control*, Vol. 37, No. 11, pp. 1746-1757, (1992).

[8] Astolfi, Alessandro, "Discontinuous control of nonholonomic systems." *Systems & control letters*, Vol. 27, No. 1 pp. 37-45, (1996).

[9] Farzad Pourboghrat, "Exponential stabilization of nonholonomic mobile robots." *Computers & Electrical*

Engineering, Vol. 28, No. 5, pp. 349-359, (2002).

[10] Dong Wenjie, W. Liang Xu, and Wei Huo, "Trajectory tracking control of dynamic non-holonomic systems with unknown dynamics." *International Journal of Robust and Nonlinear Control*, Vol. 9, No. 13, pp. 905-922, (1999).

[11] Ge Shuzhi Sam, J. Wang, Tong Heng Lee, and G. Y. Zhou, "Adaptive robust stabilization of dynamic nonholonomic chained systems." *Journal of Field Robotics*, Vol. 18, No. 3, pp. 119-133, (2001).

[12] Kim, Min-Soeng, Jin-Ho Shin, Sun-Gi Hong, and Ju-Jang Lee, "Designing a robust adaptive dynamic controller for nonholonomic mobile robots under modeling uncertainty and disturbances." *Mechatronics*, Vol. 13, No. 5, pp. 507-519, (2003).

[13] Dong Wenjie, and K-D. Kuhnert, "Robust adaptive control of nonholonomic mobile robot with parameter and nonparameter uncertainties." *IEEE Transactions on Robotics*, Vol. 21, No. 2, pp. 261-266, (2005).

[14] B. L. Ma, and S. K. Tso, "Robust discontinuous exponential regulation of dynamic nonholonomic wheeled mobile robots with parameter uncertainties." *International Journal of Robust and Nonlinear Control*, Vol. 18, No. 9, pp. 960-974, (2008).

[15] Markus Mauder, "Robust tracking control of nonholonomic dynamic systems with application to the bi-steerable mobile robot," *Automatica*, Vol. 44, No. 10, pp. 2588-2592, (2008).

[16] Chih-Yang Chen, S. Li, Tzuu-Hseng, Ying-Chieh Yeh, and Cha-Cheng Chang, "Design and implementation of an adaptive sliding-mode dynamic controller for wheeled mobile robots." *Mechatronics*, Vol. 19, No. 2 pp.156-166, (2009).

[17] Asghar Khanpoor, Ali Keymasi Khalaji, and S. Ali A. Moosavian "Modeling and control of an underactuated tractor–trailer wheeled mobile robot." *Robotica*, pp. 35-12, pp. 2297-2318, (2017).

[18] Ali Keymasi Khalaji, and S. Ali A. Moosavian." Switching control of a tractor-trailer wheeled robot. " *International Journal of Robotics and Automation*, Vol. 30, No. 2, pp.1-9 (2015).

[19] Ali Keymasi Khalaji, and S. Ali A. Moosavian, "Modified transpose Jacobian control of a tractor-trailer wheeled robot." *Journal of Mechanical Science and Technology*, Vol. 29, No. 9, pp. 3961-3969, (2015).

[20] Ebrahim H. Mamdani, and Sedrak Assilian, "An experiment in linguistic synthesis with a fuzzy logic controller." *International journal of man-machine studies*, Vol. 7, No. 1, pp. 1-13, (1975).

How to cite this paper:

Mohammad Hossein Falsafi, Khalil Alipour and Bahram Tarvirdizadeh, "Fuzzy motion control for wheeled mobile robots in real-time" *Journal of Computational and Applied Research in Mechanical Engineering*, Vol. 8, No. 2, pp. 133-144, (2019).

DOI: 10.22061/jcarme.2018.2204.1205

URL: http://jcarme.sru.ac.ir/?_action=showPDF&article=809